Report

Current Biology

Figure-Ground Modulation in the Human Lateral Geniculate Nucleus Is Distinguishable from Top-Down Attention

Highlights

- Orientation-defined figures yield enhanced responses in the human LGN
- This figure enhancement is distinct from effects of top-down attention
- Enhancement persists with dichoptic presentation, suggesting a feedback mechanism

Authors

Sonia Poltoratski, Alexander Maier, Allen T. Newton, Frank Tong

Correspondence

sonia09@stanford.edu

In Brief

The lateral geniculate nucleus (LGN) relays information from the retina to primary visual cortex but is minimally sensitive to visual features. Using high-field fMRI at 7 Tesla, Poltoratski et al. show that this structure responds to perceptual figures in a manner consistent with a mechanism of automatic, contextually-rich corticothalamic feedback.

Poltoratski et al., 2019, Current Biology *29*, 1–7
June 17, 2019
https://doi.org/10.1016/j.cub.2019.04.068

CellPress

Current Biology
Report

Figure-Ground Modulation in the Human Lateral Geniculate Nucleus Is Distinguishable from Top-Down Attention

Sonia Poltoratski,[1,2,5,*] Alexander Maier,[1,2] Allen T. Newton,[3,4] and Frank Tong[1,2]
[1]Department of Psychology, Vanderbilt University, Nashville, TN 37240, USA
[2]Vanderbilt Vision Research Center, Vanderbilt University, Nashville, TN 37240, USA
[3]Department of Radiology & Radiological Sciences, Vanderbilt University, Nashville, TN 37240, USA
[4]Vanderbilt University Institute of Imaging Science, Nashville, TN 37240, USA
[5]Lead Contact
*Correspondence: sonia09@stanford.edu
https://doi.org/10.1016/j.cub.2019.04.068

SUMMARY

Nearly all of the information that reaches the primary visual cortex (V1) of the brain passes from the retina through the lateral geniculate nucleus (LGN) of the thalamus. Although the LGN's role in relaying feedforward signals from the retina to the cortex is well understood [1, 2], the functional role of the extensive feedback it receives from the cortex has remained elusive [3–6]. Here, we investigated whether corticothalamic feedback may contribute to perceptual processing in the LGN in a manner that is distinct from top-down effects of attention [7–10]. We used high-resolution fMRI at 7 Tesla to simultaneously measure responses to orientation-defined figures in the human LGN and V1. We found robust enhancement of perceptual figures throughout the early visual system, which could be distinguished from the effects of covert spatial attention [11–13]. In a second experiment, we demonstrated that figure enhancement occurred in the LGN even when the figure and surrounding background were presented dichoptically (i.e., to different eyes). As binocular integration primarily occurs in V1 [14, 15], these results implicate a mechanism of automatic, contextually sensitive feedback from binocular visual cortex underlying figure-ground modulation in the LGN. Our findings elucidate the functional mechanisms of this core function of the visual system [16–18], which allows people to segment and detect meaningful figures in complex visual environments. The involvement of the LGN in this rich, contextually informed visual processing—despite showing minimal feedforward selectivity for visual features [19, 20]—underscores the role of recurrent processing at the earliest stages of visual processing.

RESULTS

Figure Enhancement in the LGN and V1 Is Not Contingent on Directed Attention

We investigated the functional role of the lateral geniculate nucleus (LGN) and primary visual cortex (V1) in figure-ground processing, comparing fMRI responses to perceptual figures that were cued to be attended or ignored. Recent studies of awake-behaving monkeys have found that figure enhancement effects in V1 are severely attenuated in tasks that require attending away from the figure [11], raising the question of whether figure enhancement arises from an automatic perceptual process in the early visual system or whether it reflects a byproduct of covert spatial attention [12, 13].

In the first experiment, observers maintained fixation while viewing two lateralized figures, which consisted of oriented texture patches presented against a textured background (Figure 1A). The figures and background were dynamically regenerated every 200 ms to strongly activate the visual system. On each stimulus block, one patch was congruent in orientation with the background texture (i.e., collinear), whereas the other was incongruent (i.e., orthogonal) with the background and thereby evoked a stronger percept of a figure. By contrasting the incongruent and congruent figure conditions, we could mitigate the contribution of low-level stimulus differences that would otherwise result if one compared a figure to a uniform background, including local edge effects.

A central cue indicated whether the observer should covertly attend to the left or right texture patch to monitor for a brief increase (200 ms) in that figure's spatial frequency. The changes occurred randomly and independently at both figure locations, and observers were instructed to selectively attend and respond to the cued figure. This manipulation of spatial attention allowed us to determine whether figure enhancement occurs for both attended and unattended stimuli, as would be expected for an automatic, perceptually informed type of feedback.

Results are shown in Figure 1: figure enhancement, or greater neural responses to incongruent than to congruent figures, was evident both in V1 ($F(1, 6) = 23.3$, $p = 0.003$) and in the LGN ($F(1, 6) = 21.2$, $p = 0.0037$). We also observed stronger responses for attended figures than unattended figures (LGN: $F(1, 6) = 19.6$,

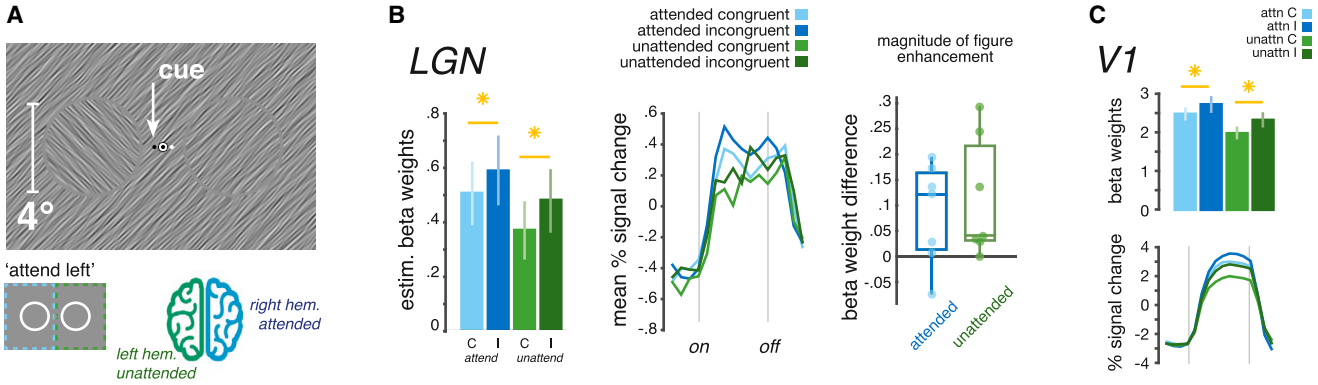

Figure 1. Figure Enhancement in the LGN and V1 Is Not Contingent on Directed Attention

(A) Example of display from Experiment 1, in which a small cue directed participants to attend to one of two lateralized figure regions. This design allowed simultaneous measurement of responses to an attended and unattended figure region. Displays consisted of bandpass-filtered oriented noise and were regenerated every 200 ms for the duration of each 16-s stimulus block. A 0.15° grayscale gap separated both figures from the background.

(B) Left: Average fMRI responses in the LGN based on estimated beta weights. Error bars depict ± 1 SEM across participants (n = 7), and asterisks denote significant t differences between experimental conditions at a threshold of $p < 0.05$. Center: time course of fMRI activity in units of mean percent signal change, shown relative to the stimulus onset and offset (gray vertical lines) for each condition. Right panel: the magnitude of figure enhancement (incongruent minus congruent orientation betas) in the LGN in both attended and unattended conditions. Circles indicate individual participant data.

(C) Results for area V1.

See also Figures S1 and S3 and Video S1.

p = 0.004; V1: $F(1, 6) = 48.5$, $p = 4.4\times10^{-4}$), indicating robust attentional modulation of early visual responses. Notably, these effects of figure enhancement occurred in the LGN and V1 not only when the observer attended to the figure (LGN: one-tailed $t(6) = 2.3$, p = 0.032; *V1:* $t(6) = 2.7$, p = 0.017) but also when spatial attention was directed to the opposite hemifield (LGN: $t(6) = 2.5$, p = 0.023; V1: $t(6) = 5.0$, p = 0.0013), with no evidence of an interaction effect (LGN: $F(1, 6) = 0.15$, p = 0.71; V1: $F(1, 6) = 0.87$, p = 0.39). Although participants were better at detecting task-relevant changes to incongruent figures than to congruent figures (89% versus 80%; $t(6) = 4.2$, p = 0.0058), a behavioral control experiment (Figure S2) indicated that participants' exogenous attention was no more likely to be attracted by unattended (or deprioritized) incongruent figures than by congruent ones. These fMRI results imply that covert spatial attention does not need to be directed at a particular figure region for enhancement to occur; instead, these effects of figure enhancement in the LGN and V1 can be attributed to more automatic perceptual processes.

The Role of Binocular Corticothalamic Feedback in LGN Figure-Ground Modulation

In a second experiment, we capitalized on the known anatomical organization of the binocular visual system to evaluate whether corticothalamic feedback to the LGN, rather than feedforward processing, was the likely cause of figure enhancement at this very early stage of the visual hierarchy. Inputs from the two eyes project to distinct monocular layers of the LGN and are subsequently integrated in the primary visual cortex [14, 15, 21]. Thus, should figure enhancement persist in the LGN while the figure and the surrounding background are shown to two different eyes, such LGN modulation can be attributed to corticothalamic feedback from V1, rather than feedforward processing in the LGN. Moreover, dichoptic presentation avoids the potential impact of stimulus edge effects that can arise at the boundary between two visual patterns (cf. Figure 1A), as such abutting texture-defined edges were not present in the stimulus visible to either eye.

In Experiment 2A, observers were presented with figures and background to either the same eye or to different eyes (Figure 2). Participants performed a fixation-monitoring task throughout the experiment and had to monitor for brief changes in fixation contrast. Thus, the lateral figures were not task-relevant to participants at any point in the study.

The results of monocular figure-ground presentation in the LGN were highly consistent with the findings in Experiment 1. We found robust effects of figure enhancement in the LGN ($F(1, 7) = 15.6$, p = 0.006) across the two presentation conditions, with no main effect of dichoptic versus monoptic presentation ($F(1, 7) = 0.33$, p = 0.58) or any evidence of an interaction effect ($F(1, 7) = 0.23$, p = 0.65). Thus, the results of Experiment 2A replicated the findings of Experiment 1 in that unattended figures were enhanced when the figure and surround were presented to the same eye ($t(7) = 3.1$, p = 0.0083). More importantly, figure enhancement persisted in the LGN when the figure and background were presented to different eyes ($t(7) = 2.3$, p = 0.028), implicating a mechanism of corticothalamic feedback for these contextually sensitive responses in the LGN. In V1, we again found strong effects of figure enhancement ($F(1, 7) = 27.0$, p = 0.0013) when the stimuli were presented both monoptically ($t(7) = 5.7$, p = 0.0004) and dichoptically ($t(7) = 4.1$, p = 0.0022); here, stronger enhancement was observed under monoptic presentation (interaction effect in V1: $F(1, 7) = 34.2$, $p = 6.3\times10^{-4}$).

Although Experiment 1 suggested that figure enhancement in the LGN is not contingent on directed attention to the figure, we considered whether the central fixation task in Experiment 2A was sufficiently difficult to discourage participants from concurrently attending to the lateral figures, as behavioral performance was high (mean accuracy 95.3%, standard error 0.94%). We therefore sought to replicate and extend these findings in a

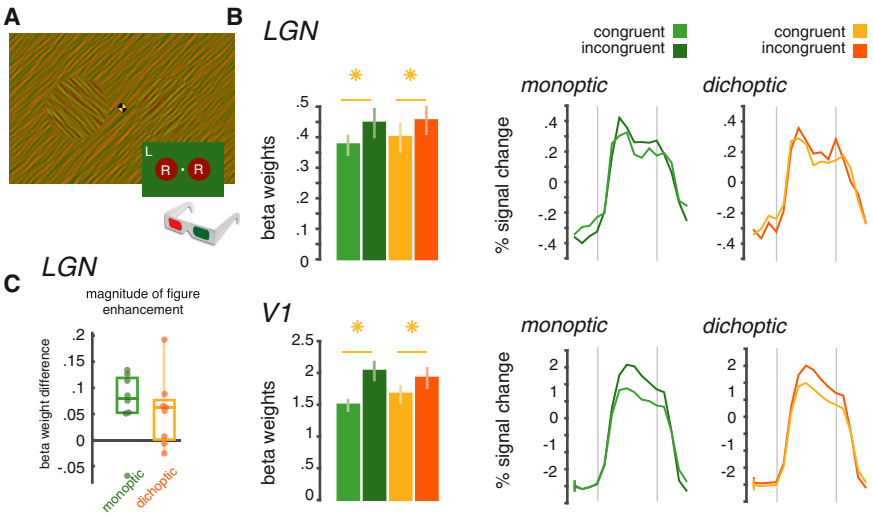

Figure 2. The Role of Binocular Corticothalamic Feedback in LGN Figure-Ground Modulation

Design and results of Experiment 2A (n = 8), in which the figure and surround stimuli were presented either to the same eye or to different eyes. Plotting follows the conventions of Figure 1.

(A) Example dichoptic stimuli used in Experiment 2A; when viewed through red/green anaglyph glasses, as shown, the two lateralized figures are visible to the right eye, while the surround is visible to the left.

(B) Estimated Beta weights and time courses across conditions in Experiment 2A.

(C) The magnitude of figure enhancement in the dichoptic and monoptic conditions for LGN. Circles represent individual participants.

See also Figure S3 and Video S2.

follow-up experiment that required participants to perform a challenging letter recognition task at central fixation (mean accuracy, 56.7%, SE 5.7%).

In Experiment 2B, participants had to monitor a rapidly presented continuous stream of letters (6.25 letters/second) and report whenever a "J" or "K" briefly appeared (on average, once per 1.6 s) by pressing one of two corresponding buttons on a response box. Participants performed this challenging task, which required sustained attention, throughout the entire ~4.5 min experimental run (Figure 3A; chance performance is 0%). Critically, behavioral performance in the scanner was unaffected by the onset or offset of the lateral figures, implying that these task-irrelevant figures did not distract participants from performing their central task (Figures 3A and 3B; stimulus on versus off $t(5) = 0.21$, $p = 0.84$). Moreover, a behavioral control experiment performed outside of the scanner indicated that participants could successfully attend to the letter monitoring task (80.7% accuracy, SE 2.29%) but performed at chance-level when they were occasionally cued to report whether the incongruent figure appeared to the left or right of fixation (mean accuracy 52.8%, chance level 50%, $t(5) = 0.42$, $p = 0.69$; Figure S3).

Experiment 2B revealed consistent effects of figure enhancement in the LGN (Figure 3B; $F(1, 5) = 10.5$, $p = 0.022$) when the stimuli were presented both monoptically ($t(5) = 2.3$, $p = 0.035$) and dichoptically ($t(5) = 3.1$, $p = 0.013$). There was no evidence of an interaction effect between figure enhancement and ocular presentation ($F(1, 5) = 0.02$, $p = 0.90$). Primary visual cortex likewise showed enhancement both in monoptic and dichoptic conditions ($F(1, 5) = 24.1$, $p = 0.005$; t's (5) > 4.6, p's < 0.003; main effect of figure enhancement: $F(1, 5) = 24.06$, $p = 0.0045$; interaction effect: $F(1, 5) = 2.52$, $p = 0.17$). Thus, we find compelling evidence of figure enhancement in the LGN, even when figure and surround are presented to different eyes and even when participants performed an attentionally demanding task away from the figures.

What neural processes can readily account for figure-ground modulation in the LGN, allowing for contextual sensitivity to orientation differences and the ability to integrate information across the two eyes? Given that the feedforward response properties of the LGN are quite rudimentary, we believe these effects are unlikely to originate within the structure itself. Both magnocellular and parvocellular neurons in the LGN are monocularly driven, and the proportion of LGN neurons that exhibit binocular responses is estimated to be very low (~3%) [15, 22–24]. Additionally, single-unit recordings in anesthetized monkeys have failed to find evidence of orientation-tuned spatial interactions [2, 19]. (That said, more research is needed to determine the full range of neural computations that occur within the LGN.)

Information from V1, as well as V2, can be propagated back to the LGN via distinct feedback projections [3]. In primates, V1 is widely considered the first stage of the visual hierarchy in which information from the two eyes is combined and processed binocularly [14]; indeed, layer 6 of V1, where the majority of corticothalamic feedback originates, consists mostly of binocularly responsive neurons [25]. Contextual sensitivity to orientation, including pervasive effects of orientation-tuned surround suppression [26, 27], is likewise well-documented in V1. Given these properties and the multiple positive reports of figure-ground modulation in V1 [11, 16, 17], corticothalamic feedback provides a parsimonious account for the figure enhancement we observed in the LGN.

Could other structures that project to the LGN bear responsibility for figure-ground effects? Notably, the superior colliculus (SC) contains a large percentage of binocular neurons [28, 29] that project to the LGN [30] and is heavily involved in orienting attention and planning saccades to behaviorally relevant objects. However, it is not evident how the SC would process the unattended, behaviorally irrelevant figures for which we observed enhancement or whether it can encode relative differences in orientation. Although orientation selectivity in the SC has been found in the rodent [31], this tuning is absent or weak in the primate [28, 32, 33], comparable to the coarse orientation preferences found in the primate LGN [34].

DISCUSSION

The patterns of light that form on the retinae are not perceived as a continuous two-dimensional array; instead, we experience a parsed landscape of meaningful figures, surfaces, and objects. Visual features, such as orientation, color, and binocular disparity,

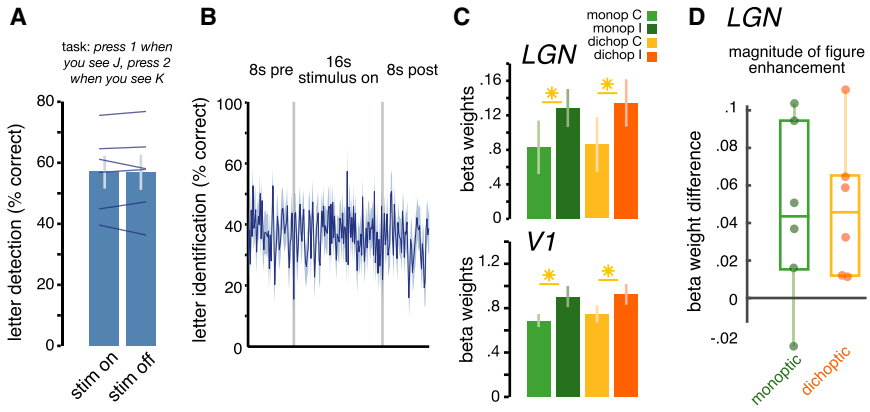

Figure 3. Dichoptic Figure Enhancement when Attention Is Strongly Engaged Elsewhere

Behavioral and imaging results of Experiment 2B (n = 6), in which participants performed a challenging letter detection task while viewing figures. Plotting follows the conventions of Figure 2.

(A) Performance on the J/K detection task, both when the oriented noise stimuli were on and off the screen. Overlaid lines indicate individual subject performance.

(B) Performance across subjects relative to the onset and offset of stimulus blocks; bins correspond to 160 ms letter presentations.

(C) Mean Beta estimates show significant figure enhancement in LGN and V1 under both presentation conditions.

(D) The magnitude of figure enhancement in LGN. Circles represent individual participants.

See also Figures S2 and S3 and Video S3.

provide powerful cues for the segmentation of visual objects. Figures defined by these features have been found to evoke enhanced responses from neurons recorded in the V1 [16, 17]. Two distinct mechanisms have been identified for the separation of figure from ground: an initial boundary detection and a subsequent region-growing mechanism that groups portions of the image that share features. Edge detection of orientation-defined figures is thought to arise from feature-tuned suppression and can act very rapidly [26, 35]. Enhancement within the figure, however, emerges later in time, suggesting that feedback propagates from higher to lower visual areas [36, 37], due to either automatic perceptual processing or a mechanism of spatial attention [11, 12, 38, 39]. In support of a dual-stage segmentation process, human performance at discriminating figures is well described by models that instantiate both border detection and a subsequent filling-in process [40, 41].

Our findings shed light on the functional role of feedback to the LGN in visual perception and figure-ground processing. We provide novel evidence that figure-ground modulation in the LGN operates in a manner that is consistent with automatic perceptual processing mediated by corticothalamic feedback. Specifically, we find that figure-ground modulation in the human visual cortex and LGN occurs (1) in the absence of directed attention to the figure and (2) even when the figure and surround are presented to different eyes, as predicted by top-down modulation from the binocular visual cortex.

The LGN of the thalamus receives a large number of feedback projections from V1 [3] and constitutes the earliest stage of the visual hierarchy that can be modulated by top-down feedback [7–10]. Studies of the primate visual system have generally found that the LGN has minimal feature selectivity: though the LGN may inherit some weak orientation biases from the retina [19, 20, 42], it demonstrates little specificity or tuning in its extra-classical receptive field properties [2, 19]. However, studies of anesthetized animals find that orientation-tuned V1 neurons send spatially structured feedback signals to the LGN in a manner that corresponds with the structure of their oriented receptive fields [6]. In this respect, even if individual LGN neurons show little orientation tuning, the retinotopic pattern of feedback modulation in the LGN could potentially be informed by orientation processing in the early visual cortex [21]. Recent neuroimaging work from our lab has shown that orientation information can be decoded from fMRI response patterns in the LGN and that these modest but reliable orientation-biased responses can be modulated by top-down attention [9]. The current study shows that feedback can likewise carry higher-order perceptual information from the visual cortex to the LGN, as responses to the figure region are modulated by the relative orientation of the figure and the surround. This supports a recurrent model of processing in the very early visual system [43], in which V1 neurons can interact via feedback connections with the LGN to effectively increase the gain of visual responses to relevant features or locations [44–47]. Our study may also suggest a spatial dependency of this type of gain enhancement, as we previously found no evidence of response enhancement in the LGN to a uniquely oriented grating presented among an array of gratings (grating size 1°, gap separation 1.8°), while robust enhancement occurred in the visual cortex [48]. In the present work, LGN enhancement occurred when the figure and surround abutted each other closely (0.15° gap separation), suggesting that figure enhancement is distinguishable from more long-range contextual effects [49–52].

Neural theories of predictive coding [53, 54] have long posited that topographically organized feedforward-feedback connections between the LGN, V1, and higher cortical visual areas are essential for the computations performed by the visual system. After the initial feedforward sweep of visual responses, neurons in higher areas with large receptive fields can process visual information in a more global and abstracted manner and send predictions regarding the patterns of activity they receive to the lower area that provides their input. Predictions and actual inputs are then compared in the lower area, and any residual errors in these local predictions are then propagated forward from the lower area to the higher area for further processing. This process results in more efficient coding and lower firing rates over time. A potential implication of this theory is that top-down predictions from higher-level visual areas with larger integration windows might propagate to the lowest possible site of the visual hierarchy, modulating the response of the LGN to figural regions that differ in appearance from the adjacent background. Recent implementations of predictive coding in deep neural networks

suggest that error signals associated with detecting a figure or object in a natural scene can lead to spatially widespread effects, even in the lowest layers of the network where the receptive fields of individual units are extremely small [55]. The current work provides novel evidence that concurs with the anticipated effects of predictive coding in the LGN.

Our study further demonstrates that figure enhancement occurs even when spatial attention is directed away from the figure. Given that the LGN can be reliably modulated by spatial attention [8–10, 48], it is important to control for potentially confounding effects of attentional modulation in studies of figure-ground perception. In a recent study of monkeys trained to saccade to motion-defined figures, promising effects of figure-ground modulation were observed in the LGN [13]. However, this study could not distinguish whether modulatory effects were attributable to automatic perceptual processes or to effects of spatial attention directed to the figure [11, 12, 56]. This distinction can be particularly difficult to make in animal studies that rely on reward-based training paradigms to encourage the animal to look at a perceptual figure, as such training is known to alter the value-driven attentional capture of trained stimuli [57, 58]. Our results provide compelling evidence that figure-ground modulation is an automatic, perceptually driven function of the early visual system.

Our findings contribute to a growing body of evidence suggesting that even at early stages, perception involves much more than simple feedforward processing along the visual hierarchy. In addition to top-down modulation by attention, responses at the earliest stages of the visual system are altered by complex shape and figure processing typically attributed to higher-order areas [17, 18, 37, 43, 59, 60]. Our demonstration of automatic feedback modulation in the LGN evoked by perceptual figures suggests that recurrent processes may underlie core aspects of vision across all of its processing stages.

STAR★METHODS

Detailed methods are provided in the online version of this paper and include the following:

- KEY RESOURCES TABLE
- CONTACT FOR REAGENT AND RESOURCE SHARING
- EXPERIMENTAL MODEL AND SUBJECT DETAILS
  - Participants
- METHOD DETAILS
  - Stimuli and Design
  - fMRI scanning parameters
  - ROI localization
- QUANTIFICATION AND STATISTICAL ANALYSIS
- DATA AND SOFTWARE AVAILABILITY

SUPPLEMENTAL INFORMATION

Supplemental Information can be found online at https://doi.org/10.1016/j.cub.2019.04.068.

ACKNOWLEDGMENTS

We thank Devin McCormack and Malerie MacDowell for assistance with data collection and Drs. Randolph Blake and Sam Ling for invaluable discussion.

This work was supported by US National Institutes of Health (NIH) grants R01-EY029278 (F.T.), R01-EY027402 (A.M.), P30-EY008126, and fellowship T32-EY007135.

AUTHOR CONTRIBUTIONS

S.P., A.M., and F.T. conceived the study; S.P., A.N., and F.T. designed the fMRI experiments; S.P. collected and analyzed the data; and all authors wrote the manuscript.

DECLARATION OF INTERESTS

The authors declare no competing interests.

Received: September 18, 2018
Revised: March 20, 2019
Accepted: April 26, 2019
Published: June 6, 2019

REFERENCES

1. Hubel, D.H., and Wiesel, T.N. (1961). Integrative action in the cat's lateral geniculate body. J. Physiol. *155*, 385–398.
2. Usrey, W.M., and Alitto, H.J. (2015). Visual Functions of the Thalamus. Annu Rev Vis Sci *1*, 351–371.
3. Briggs, F., Kiley, C.W., Callaway, E.M., and Usrey, W.M. (2016). Morphological Substrates for Parallel Streams of Corticogeniculate Feedback Originating in Both V1 and V2 of the Macaque Monkey. Neuron *90*, 388–399.
4. Briggs, F., and Usrey, W.M. (2011). Corticogeniculate feedback and visual processing in the primate. J. Physiol. *589*, 33–40.
5. Saalmann, Y.B., and Kastner, S. (2011). Cognitive and perceptual functions of the visual thalamus. Neuron *71*, 209–223.
6. Wang, W., Jones, H.E., Andolina, I.M., Salt, T.E., and Sillito, A.M. (2006). Functional alignment of feedback effects from visual cortex to thalamus. Nat. Neurosci. *9*, 1330–1336.
7. McAlonan, K., Cavanaugh, J., and Wurtz, R.H. (2008). Guarding the gateway to cortex with attention in visual thalamus. Nature *456*, 391–394.
8. O'Connor, D.H., Fukui, M.M., Pinsk, M.A., and Kastner, S. (2002). Attention modulates responses in the human lateral geniculate nucleus. Nat. Neurosci. *5*, 1203–1209.
9. Ling, S., Pratte, M.S., and Tong, F. (2015). Attention alters orientation processing in the human lateral geniculate nucleus. Nat. Neurosci. *18*, 496–498.
10. Schneider, K.A., and Kastner, S. (2009). Effects of sustained spatial attention in the human lateral geniculate nucleus and superior colliculus. J. Neurosci. *29*, 1784–1795.
11. Poort, J., Raudies, F., Wannig, A., Lamme, V.A.F., Neumann, H., and Roelfsema, P.R. (2012). The role of attention in figure-ground segregation in areas V1 and V4 of the visual cortex. Neuron *75*, 143–156.
12. Rossi, A.F., Desimone, R., and Ungerleider, L.G. (2001). Contextual modulation in primary visual cortex of macaques. J. Neurosci. *21*, 1698–1709.
13. Jones, H.E., Andolina, I.M., Shipp, S.D., Adams, D.L., Cudeiro, J., Salt, T.E., and Sillito, A.M. (2015). Figure-ground modulation in awake primate thalamus. Proc. Natl. Acad. Sci. USA *112*, 7085–7090.
14. Hubel, D.H., and Wiesel, T.N. (1977). Ferrier lecture. Functional architecture of macaque monkey visual cortex. Proc. R. Soc. Lond. B Biol. Sci. *198*, 1–59.
15. Dougherty, K., Schmid, M.C., and Maier, A. (2019). Binocular response modulation in the lateral geniculate nucleus. J. Comp. Neurol. *527*, 522–534.
16. Lamme, V.A. (1995). The neurophysiology of figure-ground segregation in primary visual cortex. J. Neurosci. *15*, 1605–1615.

17. Zipser, K., Lamme, V.A., and Schiller, P.H. (1996). Contextual modulation in primary visual cortex. J. Neurosci. *16*, 7376–7389.
18. Qiu, F.T., and von der Heydt, R. (2005). Figure and ground in the visual cortex: v2 combines stereoscopic cues with gestalt rules. Neuron *47*, 155–166.
19. Alitto, H.J., and Usrey, W.M. (2008). Origin and dynamics of extraclassical suppression in the lateral geniculate nucleus of the macaque monkey. Neuron *57*, 135–146.
20. Suematsu, N., Naito, T., Miyoshi, T., Sawai, H., and Sato, H. (2013). Spatiotemporal receptive field structures in retinogeniculate connections of cat. Front. Syst. Neurosci. *7*, 103.
21. Briggs, F., and Usrey, W.M. (2008). Emerging views of corticothalamic function. Curr. Opin. Neurobiol. *18*, 403–407.
22. Zeater, N., Cheong, S.K., Solomon, S.G., Dreher, B., and Martin, P.R. (2015). Binocular Visual Responses in the Primate Lateral Geniculate Nucleus. Curr. Biol. *25*, 3190–3195.
23. Marrocco, R.T., McClurkin, J.W., and Young, R.A. (1982). Modulation of lateral geniculate nucleus cell responsiveness by visual activation of the corticogeniculate pathway. J. Neurosci. *2*, 256–263.
24. Rodieck, R.W., and Dreher, B. (1979). Visual suppression from nondominant eye in the lateral geniculate nucleus: a comparison of cat and monkey. Exp. Brain Res. *35*, 465–477.
25. Lund, J.S., and Boothe, R.G. (1975). Interlaminar connections and pyramidal neuron organisation in the visual cortex, area 17, of the Macaque monkey. J. Comp. Neurol. *159*, 305–334.
26. Bair, W., Cavanaugh, J.R., and Movshon, J.A. (2003). Time course and time-distance relationships for surround suppression in macaque V1 neurons. J. Neurosci. *23*, 7690–7701.
27. Shushruth, S., Nurminen, L., Bijanzadeh, M., Ichida, J.M., Vanni, S., and Angelucci, A. (2013). Different orientation tuning of near- and far-surround suppression in macaque primary visual cortex mirrors their tuning in human perception. J. Neurosci. *33*, 106–119.
28. Moors, J., and Vendrik, A.J. (1979). Responses of single units in the monkey superior colliculus to stationary flashing stimuli. Exp. Brain Res. *35*, 333–347.
29. Marrocco, R.T., and Li, R.H. (1977). Monkey superior colliculus: properties of single cells and their afferent inputs. J. Neurophysiol. *40*, 844–860.
30. Stepniewska, I., Qi, H.X., and Kaas, J.H. (1999). Do superior colliculus projection zones in the inferior pulvinar project to MT in primates? Eur. J. Neurosci. *11*, 469–480.
31. Wang, L., Sarnaik, R., Rangarajan, K., Liu, X., and Cang, J. (2010). Visual receptive field properties of neurons in the superficial superior colliculus of the mouse. J. Neurosci. *30*, 16573–16584.
32. Goldberg, M.E., and Wurtz, R.H. (1972). Activity of superior colliculus in behaving monkey. I. Visual receptive fields of single neurons. J. Neurophysiol. *35*, 542–559.
33. Chen, C.-Y., and Hafed, Z.M. (2018). Orientation and Contrast Tuning Properties and Temporal Flicker Fusion Characteristics of Primate Superior Colliculus Neurons. Front. Neural Circuits *12*, 58.
34. Xu, X., Ichida, J., Shostak, Y., Bonds, A.B., and Casagrande, V.A. (2002). Are primate lateral geniculate nucleus (LGN) cells really sensitive to orientation or direction? Vis. Neurosci. *19*, 97–108.
35. Nothdurft, H.C., Gallant, J.L., and Van Essen, D.C. (1999). Response modulation by texture surround in primate area V1: correlates of "popout" under anesthesia. Vis. Neurosci. *16*, 15–34.
36. Self, M.W., van Kerkoerle, T., Supèr, H., and Roelfsema, P.R. (2013). Distinct roles of the cortical layers of area V1 in figure-ground segregation. Curr. Biol. *23*, 2121–2129.
37. Poort, J., Self, M.W., van Vugt, B., Malkki, H., and Roelfsema, P.R. (2016). Texture Segregation Causes Early Figure Enhancement and Later Ground Suppression in Areas V1 and V4 of Visual Cortex. Cereb. Cortex *26*, 3964–3976.
38. Marcus, D.S., and Van Essen, D.C. (2002). Scene segmentation and attention in primate cortical areas V1 and V2. J. Neurophysiol. *88*, 2648–2658.
39. Friedman, H.S., Zhou, H., and von der Heydt, R. (2003). The coding of uniform colour figures in monkey visual cortex. J. Physiol. *548*, 593–613.
40. Mumford, D., Kosslyn, S.M., Hillger, L.A., and Herrnstein, R.J. (1987). Discriminating figure from ground: the role of edge detection and region growing. Proc. Natl. Acad. Sci. USA *84*, 7354–7358.
41. Wolfson, S.S., and Landy, M.S. (1998). Examining edge- and region-based texture analysis mechanisms. Vision Res. *38*, 439–446.
42. Schall, J.D., Perry, V.H., and Leventhal, A.G. (1986). Retinal ganglion cell dendritic fields in old-world monkeys are oriented radially. Brain Res. *368*, 18–23.
43. Lamme, V.A., and Roelfsema, P.R. (2000). The distinct modes of vision offered by feedforward and recurrent processing. Trends Neurosci. *23*, 571–579.
44. Sillito, A.M., Jones, H.E., Gerstein, G.L., and West, D.C. (1994). Feature-linked synchronization of thalamic relay cell firing induced by feedback from the visual cortex. Nature *369*, 479–482.
45. Bastos, A.M., Usrey, W.M., Adams, R.A., Mangun, G.R., Fries, P., and Friston, K.J. (2012). Canonical microcircuits for predictive coding. Neuron *76*, 695–711.
46. Sillito, A.M., Cudeiro, J., and Jones, H.E. (2006). Always returning: feedback and sensory processing in visual cortex and thalamus. Trends Neurosci. *29*, 307–316.
47. Bastos, A.M., Briggs, F., Alitto, H.J., Mangun, G.R., and Usrey, W.M. (2014). Simultaneous recordings from the primary visual cortex and lateral geniculate nucleus reveal rhythmic interactions and a cortical source for γ-band oscillations. J. Neurosci. *34*, 7639–7644.
48. Poltoratski, S., Ling, S., McCormack, D., and Tong, F. (2017). Characterizing the effects of feature salience and top-down attention in the early visual system. J. Neurophysiol. *118*, 564–573.
49. Joo, S.J., Boynton, G.M., and Murray, S.O. (2012). Long-range, pattern-dependent contextual effects in early human visual cortex. Curr. Biol. *22*, 781–786.
50. Nurminen, L., and Angelucci, A. (2014). Multiple components of surround modulation in primary visual cortex: multiple neural circuits with multiple functions? Vision Res. *104*, 47–56.
51. Beck, D.M., and Kastner, S. (2005). Stimulus context modulates competition in human extrastriate cortex. Nat. Neurosci. *8*, 1110–1116.
52. Zhang, X., Zhaoping, L., Zhou, T., and Fang, F. (2012). Neural activities in v1 create a bottom-up saliency map. Neuron *73*, 183–192.
53. Rao, R.P., and Ballard, D.H. (1999). Predictive coding in the visual cortex: a functional interpretation of some extra-classical receptive-field effects. Nat. Neurosci. *2*, 79–87.
54. Mumford, D. (1992). On the computational architecture of the neocortex. II. The role of cortico-cortical loops. Biol. Cybern. *66*, 241–251.
55. Han, K., Wen, H., Zhang, Y., Di, F., Culurciello, E., and Liu, Z. (2018). Deep Predictive Coding Network with Local Recurrent Processing for Object Recognition. arXiv, arXiv:1805.07526v2. https://arxiv.org/abs/1805.07526.
56. Knierim, J.J., and van Essen, D.C. (1992). Neuronal responses to static texture patterns in area V1 of the alert macaque monkey. J. Neurophysiol. *67*, 961–980.
57. Anderson, B.A., and Yantis, S. (2013). Persistence of value-driven attentional capture. J. Exp. Psychol. Hum. Percept. Perform. *39*, 6–9.
58. Anderson, B.A., Laurent, P.A., and Yantis, S. (2011). Value-driven attentional capture. Proc. Natl. Acad. Sci. USA *108*, 10367–10371.
59. Kok, P., and de Lange, F.P. (2014). Shape perception simultaneously up- and downregulates neural activity in the primary visual cortex. Curr. Biol. *24*, 1531–1535.

60. Meng, M., Remus, D.A., and Tong, F. (2005). Filling-in of visual phantoms in the human brain. Nat. Neurosci. *8*, 1248–1254.

61. Chen, Y., Martinez-Conde, S., Macknik, S.L., Bereshpolova, Y., Swadlow, H.A., and Alonso, J.-M. (2008). Task difficulty modulates the activity of specific neuronal populations in primary visual cortex. Nat. Neurosci. *11*, 974–982.

62. Engel, S.A., Glover, G.H., and Wandell, B.A. (1997). Retinotopic organization in human visual cortex and the spatial precision of functional MRI. Cereb. Cortex *7*, 181–192.

63. Wandell, B.A., Dumoulin, S.O., and Brewer, A.A. (2007). Visual field maps in human cortex. Neuron *56*, 366–383.

64. Kastner, S., O'Connor, D.H., Fukui, M.M., Fehd, H.M., Herwig, U., and Pinsk, M.A. (2004). Functional imaging of the human lateral geniculate nucleus and pulvinar. J. Neurophysiol. *91*, 438–448.

65. Hastings, C., Jr., Mosteller, F., and Tukey, J.W. (1947). Low moments for small samples: a comparative study of order statistics. Ann. Math. Stat. *18*, 413–426.

STAR★METHODS

KEY RESOURCES TABLE

REAGENT or RESOURCE	SOURCE	IDENTIFIER
Deposited Data		
preprocessed fMRI data	This paper	https://github.com/soniapolt/LGN-figureground
Software and Algorithms		
Freesurfer	http://surfer.nmr.mgh.harvard.edu	Version 5.1.0
FSL	https://fsl.fmrib.ox.ac.uk/fsl/fslwiki/	Version 6.0
Matlab	Mathworks	Version R2014A
custom Matlab scripts (experiments, processing)	This paper	https://github.com/soniapolt/LGN-figureground and upon request
Psychtoolbox	http://psychtoolbox.org/	Version 3

CONTACT FOR REAGENT AND RESOURCE SHARING

Further information and requests for resources and reagents should be directed to and will be fulfilled by the Lead Contact, Sonia Poltoratski (sonia09@stanford.edu).

EXPERIMENTAL MODEL AND SUBJECT DETAILS

Participants

Eight experienced human observers (five females), ages 23-31, participated in Experiment 1, eight (six females, 24-31) participated in Experiment 2A, and seven (five females, 25-32) participated in the follow-up Experiment 2B. Based on an earlier study (Poltoratski & Tong, unpublished data), where we observed figure-ground modulation in the LGN for centrally presented orientation-defined figures (Cohen's d = 1.18), we estimated that running eight participants would yield 0.90 power to detect this effect in each of the experiments in this study.

All participants provided written informed consent and received monetary compensation. All aspects of this study followed the guidelines of and were approved by the Vanderbilt University Institutional Review Board. One participant's data were excluded from Experiment 1 after an imaging artifact located over his occipital pole was evident across functional images. The remaining seven subjects (including author SP) and one new subject participated in Experiment 2A. Of these subjects, six (including author SP) and one new subject participated in Experiment 2B. Data from one participant in Experiment 2B was discarded due to excessive motion over the course of the experiment (> 8mm).

METHOD DETAILS

Stimuli and Design

In all studies, observers viewed stimulus displays showing two lateralized figures embedded in an oriented surround. The two circular figures (4° in diameter) were presented to the left and the right of central fixation at 3° eccentricity. In each stimulus block, one figure was always congruent in orientation with the surround while the other was incongruent. Stimulus displays were created using randomly generated bandpass-filtered oriented noise (0.5-4cpd, 100% contrast, 45° and 135° with an orientation bandwidth of ±10°). The experimental conditions were presented in 16s stimulus blocks, during which the oriented noise patterns were dynamically regenerated every 200ms in Experiments 1 and 2A, and every 160ms in Experiment 2B; these stimulus blocks were interspersed with 16s fixation rest blocks. A 0.15° greyscale gap encircled both figure regions to minimize potential local orientation effects associated with the physically abutting figure and surround stimuli. This concern was fully addressed in Experiments 2A/B, in which figures and surround were presented to different eyes, minimizing the possibility of very local low-level interactions.

In Experiment 1, the figure and surround stimuli were presented binocularly in greyscale (Video S1). One second before each stimulus block, the participant was presented with a central cue indicating whether the left or right figure should be attended on that block. The task-relevant cue consisted of a pair of dots (0.1°), one white and one black, that appeared to the left and to the right of fixation. Each participant was told to attend to the side indicated by one of these two dots throughout the experiment, and cue (black/white) was counterbalanced across participants.

The task required subjects to report whenever they saw a brief (200ms) change in the spatial frequency of the task-relevant figure, which shifted from 0.5-4cpd to 1.5-12cpd. These changes occurred, on average, 4 times at each figure location at randomly determined times in each 16s block; the timing of their occurrence was independently determined for each figure. Participants used a button box to make their responses in the scanner, and maintained central fixation throughout the experiment.

The experimental conditions of figure/surround orientation and attended location were fully counterbalanced and presented in randomly ordered blocks within each experimental run, which lasted approximately 4.5 min. Each participant completed 10-16 functional runs of this task. Performance was somewhat better when participants attended to incongruent figures (89%, SE 1.5%) than to congruent figures (80%, SE 3.2%; $t(6) = 4.2$, $p = .0058$). However, this behavioral difference cannot account for the stronger responses that we observed for incongruent than for congruent figures: prior research [61] predicts that modulations by task should instead lead to stronger responses for the congruent figure task, which was more difficult for participants.

In Experiment 2A, we used red/green anaglyph glasses to present the figures and the surrounding background either to the same eye or to different eyes (Video S2). Participants wore these glasses throughout the scanning session, with the red lens always placed over the right eye; thus, oriented noise specified by the red LCD component of the projector would be visible to the right eye but filtered by the lens on the left eye and vice versa. To create the colored stimuli, we presented full-contrast oriented noise (same parameters as Experiment 1) using only the red and green color channels of the projector; the green color channel was reduced from a range of 0-256 to a range of 0-200 to more closely match the apparent luminance of the red, though our experimental design did not necessitate luminance matching of the two colors. Using a photometer to measure the scanner projector, we confirmed that less than 1.5% cross-talk occurred for red/green images projected through the mismatched filter. Dichoptic stimuli consisted of red/green figure/ground or vice versa, and monoptic stimuli were either all red or all green. Colors used (and thus eye of presentation) were counterbalanced and randomized across blocks. To participants, the stimuli appeared largely achromatic; however, we acknowledge that we cannot rule out the contribution of some color differences between the figure and surround in the dichoptic condition. Future work should explore potential interactions between the defining features of the figure (e.g., orientation, color, disparity) and the response enhancement that results from such manipulations.

Throughout the experimental run, the participant's task was to detect brief (200ms) contrast decrements of the central fixation point, which was a small circular 2 x 2 checkerboard to facilitate stable fixation and vergence (as illustrated in Figure 2A). These decrements were 50% contrast in magnitude, and occurred on average 4 times per block. Participants detected these events with 95% accuracy (SE 0.94%) and performed between 12 and 16 functional runs.

The stimulus design of Experiment 2B followed that of 2A, consisting of lateralized figures monoptically or dichoptically presented through red/green anaglyph glasses (Video S3). All parameters of the oriented noise stimuli were identical except the rate at which the entire visual display was regenerated; this was changed from 200ms to 160ms to accommodate the difficult letter task. Throughout the entire experimental run, the central fixation point (0.4° diameter) contained a rapid letter stream consisting of all 26 uppercase English letters. Participants were instructed to monitor the letters, and to press one button (1, pointer finger) on the button box when they saw a 'J,' and another button (2, middle finger) when they saw a 'K.' Chance-level performance was 0% for this task, as it required both detection and identification of a variable number of brief (160ms) targets. The timing of the targets was randomized within the 272s run, but targets could not occur in the first or last 640ms of the run, nor within 320ms of a previous target. The number of targets in a run was selected stochastically such that 10% of letters were a J/K target, for an average of 167 targets per run (or 1 target every 1.62 seconds on average). Participants performed the J/K detection task with accuracy of 56.7% (SE 5.7%); if a participant's performance did not rise above 40% after 2-3 runs, the size of the fixation and letters was increased to 0.5° diameter. For one participant, an additional change was made to slow the presentation rate of the letters to 200ms to improve task accuracy. Participants reported consistent engagement in the letter detection task, and minimal awareness of the surrounding stimuli. Each participant completed 10-14 functional runs of this task.

fMRI scanning parameters

All functional data were collected at the Vanderbilt University Institute for Imaging Science research-dedicated 7Tesla Philips Achieva scanner using a quadrature transmit coil in combination with a 32-channel parallel receive coil array. BOLD activity was measured using single-shot, gradient-echo echoplanar T2*-weighted imaging, at a 2 mm isotropic voxel resolution (40 slices in Experiments 1 and 2A; 34-40 slices in Experiment 2B; TR 2000ms, TE 35ms; flip angle 63°; FOV 224 x 224; SENSE acceleration factor of 2.9; phase-encoding in AP direction). Additionally, each subject underwent a separate session of retinotopic mapping, which used a standard phase-encoded design [62] and a mapping stimulus of flashing checkerboard wedges and expanding rings. Retinotopy data were acquired using a Philips 3Tesla Intera Achieva MRI scanner equipped with an 8-channel receive coil array. The retinotopy fMRI data were collected using 3-mm isotropic resolution (TR 2s, TE 35ms, flip angle 80°, 28 slices, 192 x 192 FOV).

ROI localization

In the experimental scan session, we ran 2-4 runs of a visual localizer consisting of full-contrast flickering checkerboards at each of the two figure locations; the checkerboards were presented in 16s alternating blocks. These data were used in conjunction with a separate session of retinotopy mapping to identify cortical regions of interest in V1-hV4. Boundaries between retinotopic areas V1-hV4 were manually delineated for each participant based on reversals in the phase of the polar-angle map measurements [62, 63]. One participant in Experiment 2B lacked consistent hV4 maps, so these data are missing from the Supplemental Information analysis of hV4. These retinotopic labels were aligned to the functional space of the current experiment using FSL and Freesurfer software; this registration was checked and adjusted by hand. Subsequently, cortical regions of interest (ROIs) were selected from the conjunction of retinotopy and a statistical map of the left vs. right contrast of our functional localizer. We report results from the 100 most functionally selective voxels (defined by the *t*-statistic map) in each lateralized early visual area V1-hV4, although our reported results hold across selection criteria.

The LGN was identified on the basis of the checkerboard functional localizer as the contiguous cluster of voxels in the medial subcortex using a *t*-statistic threshold of no less than 2.3; we sought to select a maximally lateralized cluster in each hemisphere to avoid including other neighboring regions of the thalamus. The LGN is more readily activated by visual stimulation than other subcortical regions, and studies suggest that functional localizers that rely on passive viewing, as ours did, do not effectively activate the pulvinar [64]. LGN ROIs in individual subjects consisted of 23-48 voxels bilaterally in Experiment 1 (mean 37.0, SD 8.3), 19-57 voxels bilaterally in Experiment 2A (mean 37.3, SD 13.1), and 15-53 voxels bilaterally in Experiment 2B (mean 35.8, SD 13.7). An example of the localized LGN is shown in Figure S1A.

QUANTIFICATION AND STATISTICAL ANALYSIS

Data were preprocessed using FSL and Freesurfer tools (documented and freely available for download at http://surfer.nmr.mgh.harvard.edu), beginning with 3D motion correction and linear trend removal, followed by a high-pass temporal filter cutoff of 60s. Functional images were registered to a reconstructed anatomical space for each subject; this registration was first automated in FSL and then checked and corrected by hand. This allowed for the alignment of the current fMRI data to the retinotopy data, which were collected in a separate session. The functional localizer was spatially smoothed using a 1-mm Gaussian kernel; no spatial smoothing was applied to the experimental runs. Further analyses were conducted using a custom Matlab processing stream. Each voxel's intensities were normalized by the mean of the time series, converting to mean percent signal change within each run. Outliers were defined as time points for which the voxel's response measured more than 3 times its standard deviation from its mean, and were Winsorised [65]. Finally, a general linear model was fitted to the time course of each run to generate a standardized Beta weight for each stimulus block; these Beta weights were then averaged by experimental condition. For the reported analyses, average Beta values from bilateral ROIs in each subject were used.

As described in the Participants section, this experiment was designed to test for an effect of figure-ground modulation in the LGN. The critical comparisons are reported as within-subject ANOVA results, and significance is defined at $p < .05$. In Experiment 1, the main factors were attention (unattended vs. attended) and figure orientation (incongruent vs. congruent); in Experiments 2A/B, the main factors were eye presentation (monoptic vs. dichoptic) and figure orientation (incongruent vs. congruent). t tests were used to further refine our understanding of significant ANOVA results; one-tailed tests were used for comparisons for which we had a strong expectation of the directionality of the effect (e.g., attended figures producing greater responses than unattended figures, or incongruent-orientation figures producing greater responses than congruent-orientation figures); two-tailed tests were used when no such expectation was evident (e.g., the magnitude of figure enhancement when figures were presented monoptically vs. dichoptically). In addition, we used the Lilliefors test to confirm the normality of our data, which supported our use of parametric statistical testing.

DATA AND SOFTWARE AVAILABILITY

The code used to generate stimuli for the main experiments, localizer, and behavioral controls can be found at https://github.com/soniapolt/LGN-figureground. This repository also contains de-identified preprocessed fMRI data for the main experiments. Additional requests for code and data should be directed to the Lead Contact, Sonia Poltoratski (sonia09@stanford.edu).